Theory of surface-potential-mediated photorefractivelike effects in liquid crystals

V. O. Kubytskyi* and V. Y. Reshetnyak
Physics Faculty, Kyiv National Taras Shevchenko University, Prospekt Glushkova 2, Kyiv 03022, Ukraine

T. J. Sluckin
School of Mathematics, University of Southampton, Southampton SO17 1BJ, United Kingdom

S. J. Cox
School of Engineering Science, University of Southampton, Southampton SO17 1BJ, United Kingdom
(Received 28 November 2007; published 13 January 2009)

We make a phenomenological model of optical two-beam interaction in a model planar liquid crystal cell. The liquid crystal is subject to homeotropic anchoring at the cell walls, is surrounded by thin photosensitive layers, and is subject to a variable potential across the cell. These systems are often known as liquid crystal photorefractive systems. The interference between the two obliquely incident beams causes a time-independent periodic modulation in electric field intensity in the direction transverse to the cell normal. Our model includes this field phenomenologically by supposing an effect on the electric potential at the cell walls. The transverse periodic surface potential causes spatially periodic departures from a pure homeotropic texture. The texture modulation acts as a grating for the incident light. The incident light is both directly transmitted and also subject to diffraction. The lowest order diffracted beams correspond to energy exchange between the beams. We find that the degree of energy exchange can be strongly sensitive to the mean angle of incidence, the angle between the beams, and the imposed potential across the cell. We use the model to speculate about what factors optimize nonlinear optical interaction in liquid crystalline photorefractive systems.

DOI: 10.1103/PhysRevE.79.011703 PACS number(s): 61.30.−v, 42.70.Df, 42.79.Kr, 42.70.Nq

I. INTRODUCTION

It has long been known that nematic liquid crystals act as nonlinear optical media [1]. The electric fields in a strong light beam reorient the liquid crystal director. In so doing they affect the dielectric properties of the medium, and hence its light transmission and reflection. Thus the liquid crystal reacts differently to a high intensity beam than when the intensity is low. A slab of liquid crystal exhibits analogous properties when irradiated by two beams rather than by a single beam. The liquid crystal responds to the interference pattern between the beams. The result is a grating in the liquid crystal cell, which diffracts the incoming beams. The lowest order diffracted beams from each incident beam act to reinforce the other, leading to the phenomenon of beam amplification. This latter phenomenon is the subject of this paper.

In general, beam coupling is a highly nonlinear phenomenon and as such requires intense beams to manifest itself. However, it has been found experimentally that there are circumstances when beam coupling appears to occur at much lower light intensities. The device possibilities of these high beam-coupling conditions have meant that these systems have attracted much interest. Two particular interesting systems obtain when either the liquid crystal is doped by dye molecules, or when the liquid crystal cell is sandwiched between walls consisting of photoconducting material. Now free charges can play an important role in the nonlinear optics. In the former case the ions move inside the liquid crystal itself. The existence of ions in these systems has led to this phenomenon being linked with photorefraction [2]. We note also, of course, that photorefractivelike effects are not the only sources of optical nonlinearity in dye-doped liquid crystals [3,4]. In the latter case the ions affect the boundary conditions to which the liquid crystal is subject.

In this paper we consider the second of these cases—that in which the liquid crystal is surrounded by photosensitive layers. An associated feature of such systems is that the degree of beam coupling is strongly dependent on, and amplified by, a low-frequency voltage across the liquid crystal cell. In photorefractive systems moving charges lead to nonlinear optical effects. These so-called photorefractive liquid crystal systems exhibit large optical nonlinearities, at least partly because two nonlinear optical processes seem to be manifesting themselves simultaneously. This statement, however, while true, is insufficient even to give the most basic description of the physics of beamcoupling in these systems. Here we present a phenomenological model, which although by no means a complete description of the system, provides a basic framework for understanding of some of the most striking features of the experiments. The most important of these features is the observation that the largest beam-coupling effects occur when the grating period is comparable to the cell thickness.

Experimental work in photorefraction in liquid crystals dates back about decade. In the cases of interest in this paper, the effect results because a spatially modulated light field causes a modulation of the electric field either in the aligning layer itself [5–9] or in the interface between the liquid crystal (LC) and this layer [10–12]. In the first case the liquid crystal cell is lined by photoconductive aligning layers, whose electrical resistance is decreased by light irradiation. This in-

*kubba@univ.kiev.ua

creases the electric field in the liquid crystal bulk, which in turn causes a spatially modulated reorientation of the director in the cell. The effect is reversible; the induced gratings disappear when the incident light is switched off. By contrast, in the second case the photorefraction is controlled by the processes in the interface between LC and aligning surfaces. Both of these layers may be nominally insensitive to light. The resultant spatially modulated electric field induces a reorientation of the director in the bulk and a permanent grating.

Theoretical work on these systems has concentrated on extending existing photorefractive concepts, which have been developed for optically isotropic systems. In the isotropic case, the key inputs into an experiment are the cell thickness L, the light wavelength λ, the grating period Λ, and the dielectric constant ε of the medium. Kogelnik [13] developed a coupled-wave theory which can predict the response of volume holograms (i.e., thick gratings). A good review of this theory can be found in the book by Yeh [14]. Klein [15] derived a criterion for a grating to be thick, in terms of the parameter $Q=2\pi L\lambda/\Lambda^2\sqrt{\varepsilon}$. The coupled wave theory begins to give good results when $Q \geqslant 10$.

Montemezzani and Zgonik [16] have extended the Kogelnik coupled-wave theory to the case of moderately absorbing thick anisotropic materials with grating vector and medium boundaries arbitrary oriented with respect to the main axes of the optical indicatrix. The dielectric tensor modulation takes the form

$$\hat{\varepsilon} = [\varepsilon_r^0 + \varepsilon_r^1 \cos(Kr)] + i[\varepsilon_i^0 + \varepsilon_i^1 \cos(Kr + \phi)]. \quad (1)$$

The same authors have then used this formalism to consider explicity beam-coupling effects [17]. A variant of this idea has also been applied to anisotropic thin holographic media by Galstyan *et al.* [18].

The key extra piece of physics in liquid crystal cells is that the director is anchored by the cell walls. As a result the spatial modulation of the dielectric function is considerably more complicated than the Montemezzani-Zgonik form. In addition, the liquid crystal cell parameters are often in the so-called Raman-Nath regime [19,20], which corresponds to thin gratings. For thin isotropic gratings with a one-dimensional refractive index modulation, the theory is well developed (see, for example, Ref. [19]). For such a system, for example, Kojima [21] used a phase function method to understand the diffraction problem for weakly inhomogeneous anisotropic materials in the Raman-Nath regime, assuming a dielectric function spatial modulation $\varepsilon \sim \cos(\Omega t - Kx)$.

An important theoretical contribution is due to Tabiryan and Umeton [22]. These authors explicitly modeled the effect of the surface charge (and hence potential) modulation on the liquid crystal director. However, in their model, the modulated electric field is localized in the region of the surface. Furthermore they do not make any explicit predictions concerning the optical properties of the liquid crystal layers, beyond general comments that their work has significance in understanding liquid crystal optics in these situations.

In this paper we shall study the diffraction and energy transfer of two light beams intersecting in a nematic liquid crystal cell, building on the work of Tabiryan and Umeton [22]. We suppose strong homeotropic anchoring at the cell walls, and that the cell be sandwiched between two photoconductive layers. The beam-coupling can be amplified by a dc-electric field, which is applied to the cell perpendicular to the cell walls (O_z direction). The model theoretical problem we pose is partly motivated by the experiments of Korneichuk *et al.* [23], and partly by those of Kaczmarek *et al.* [8]. However, the Korneichuk experiments [23] are more oriented toward dynamical effects and omit the photoconductive layer, whereas those of Kaczmarek [8] study different anchoring conditions from those in our theoretical model.

The presence of the two beams causes a periodic lattice in the light intensity field in the cell bulk and its boundaries. In addition, the laterally periodic light intensity also causes a modulation in the dc electric field potential at the cell boundaries. This paper addresses the photorefraction problem phenomenologically.

Specifically, we consider here a restricted problem with two major caveats. First we shall not examine too closely the origin and mechanism of this modulation. We simply remark that it can and does result from different physicochemical phenomena taking place at the cell walls. Likewise in this simple approach, we shall suppose that the physics of the electric field in the liquid crystal is driven by dielectric processes, and that charge transport does not play a major role in determining director orientation or light scattering. Elsewhere we shall relax both of these constraints.

The key to understanding beam coupling in these systems lies in the following observation. The surface potential modulation produces a spatially modulated electric field. The resulting torque on the liquid crystal director distorts the initial homogeneous homeotropic alignment. The consequence is an anisotropic medium with a spatially modulated director and hence optical axis. The test beam—or the beams that write the grating—diffract from the liquid crystal cell, which now possesses a spatially modulated refractive index. One may then calculate beam diffraction and interbeam energy transfer.

The paper is organized as follows. In Sec. II we determine the electric field profile in a cell subject to a light-induced periodic modulation of the surface potential. In Sect. III we calculate the director distribution inside the liquid crystal cell subject to this spatially modulated electric field. Then in Sec. IV we present results of calculations of beam diffraction and energy transfer. Finally in Sec. V we present some brief conclusions, and focus on possible extensions of the model.

II. ELECTRIC FIELD WITHIN THE CRYSTAL SLAB

We consider two equal frequency light beams with wave numbers $\mathbf{k}_1 \approx \mathbf{k}_2$ inside the medium (see Fig. 1). These beams give rise to electric fields E_1, E_2, and intensities I_1, I_2 proportional to the squares of the respective electric fields

$$\mathbf{E}_1 = E_{10} \exp(i\mathbf{k}_1 \cdot \mathbf{r}), \quad (2)$$

$$\mathbf{E}_2 = E_{20} \exp(i\mathbf{k}_2 \cdot \mathbf{r}), \quad (3)$$

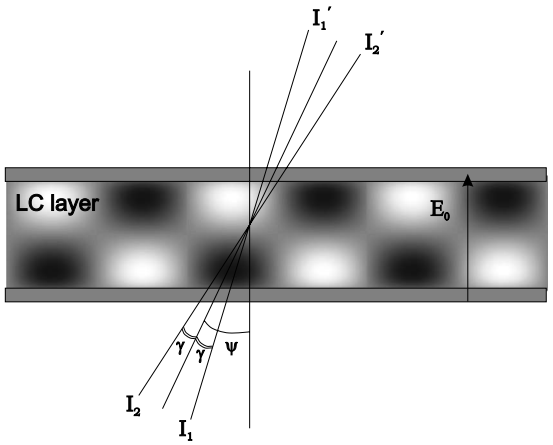

FIG. 1. Schematic picture of a two-beam coupling experiment, showing the meaning of quantities used in the paper.

$$\mathbf{k}_1 = [k \sin(\psi + \gamma), 0, k \cos(\psi + \gamma)], \tag{4}$$

$$\mathbf{k}_2 = [k \sin(\psi - \gamma), 0, k \cos(\psi - \gamma)]. \tag{5}$$

The bisector of the beams makes an angle ψ with the cell normal and $2\gamma \ll \psi$ is the angle between the beams. Initially we suppose that the scattering by the cell is weak, and thus the light transmission through the cell is close to unity.

The beams interfere in the liquid crystal slab, forming a complex intensity pattern with wave number $q = k_{1x} - k_{2x}$. In principle the pattern must be calculated self-consistently.

However, we can suppose that optical non-linear effects within the liquid crystal slab are negligible. In practice this is the case. Then it is possible to treat surface-induced and bulk-induced effects independently. In this section we focus specifically on the effect at the surfaces. At the bottom (i.e., incident) interface, the optical interference pattern takes the form

$$I(x, z = 0) = I_1 + I_2 + 2 \sum (I_1 I_2)^{1/2} \cos qx,$$

$$q = k_{1x} - k_{2x}. \tag{6}$$

Likewise, at the top substrate we have an analogous pattern, but shifted in phase with respect to the lower substrate:

$$I(x, z = L) = I_1 + I_2 + 2 \sum (I_1 I_2)^{1/2} \cos(qx + \delta),$$

$$q = k_{1x} - k_{2x}, \tag{7}$$

$$\delta = (k_{1z} - k_{2z}) L. \tag{8}$$

In the absence of the light beams, we suppose a voltage Φ_0 across the liquid crystal cell. This is a key input to the theory. In photorefractive systems the optical nonlinear effects are large and strongly amplified by a voltage across the cell. In the simple theory presented here the nonlinear effect in the absence of an external field is strictly zero.

We now make the hypothesis that the spatial distribution of light intensity induces a modulation in the surface potentials. The effect of the light beams is to modify these potentials slightly. If the surface preparation of the upper and lower surfaces is identical, then the magnitude of the surface perturbations should also be identical. The boundary conditions on the electric potential at the top and bottom substrates can now be written

$$\varphi(z = 0, x) = -\Phi_0/2 + \Phi_1 \cos qx,$$

$$\varphi(z = L, x) = \Phi_0/2 + S\Phi_1 \cos(qx + \delta). \tag{9}$$

The quantity $\Phi_1 = \alpha (I_1 I_2)^{1/2}$, where the parameter α is a phenomenological quantity, and in principle is different for each surface configuration. The parameter α can in principle be determined independently by a Frederiks experiment [34]. The quantity S could in principle take the value either +1 or −1. The phenomenological model is not precise enough to specify which of these two values is appropriate. However, different microscopic pictures can yield either value of S. We discuss this interesting point further in the Appendix. In the paper we shall suppose $S = +1$. However, we note that if $S = -1$, the theoretical development in the paper remains robust, subject to the replacement of δ by $\delta + \pi$.

We now proceed to determine the electric field potential within the liquid crystal slab. The electric field obeys the equation

$$\nabla \cdot \mathbf{D} = 0 \tag{10}$$

with $D_i = \varepsilon_{ij} E_j = [\varepsilon_\perp \delta_{ij} + (\varepsilon_\parallel - \varepsilon_\perp) n_i n_j] E_j$, where $\mathbf{n}$ is the nematic director.

We can solve Eq. (10) using relation $\mathbf{E} = -\nabla \varphi$. At this stage we note that the equations for φ and $\mathbf{n}$ must be solved self-consistently. However the liquid crystal is subject to homeotropic boundary conditions, and hence except at very strong light intensities the director is closely aligned to the direction perpendicular to the slab: $\mathbf{n} \approx \mathbf{e}_z$, and then

$$\varepsilon_\perp \frac{\partial^2 \varphi}{\partial x^2} + \varepsilon_\parallel \frac{\partial^2 \varphi}{\partial z^2} = 0. \tag{11}$$

The problem to be solved is thus Eq. (11), subject to the boundary conditions (9). This problem can be solved analytically, yielding

$$\varphi(x, z) = \Phi_0 \frac{z - L/2}{L} + \Phi_1 \left[\left\{ \cosh(\tilde{q} z) + \frac{\cos \delta - \cosh(\tilde{q} L)}{\sinh \tilde{q} L} \sinh(\tilde{q} z) \right\} \cos qx - \frac{\sin \delta}{\sinh \tilde{q} L} \sinh(\tilde{q} z) \sin qx \right], \tag{12}$$

where $\tilde{q} = \sqrt{\frac{\varepsilon_\perp}{\varepsilon_\parallel}} q$. The potential in the liquid crystal slab consists of the externally imposed voltage plus a contribution linear in the surface perturbation induced by the light-beam interference. This perturbation has the same periodicity in the direction in the cell plane as the initial perturbation. However, the behavior is complex as a result of the competing effects of the out-of-phase surface perturbations.

The resulting electric field, in addition to the imposed external field E_0 normal to the cell, has components in both the x and z directions. The contributions in the x direction are

particularly important, because they lead to director distortion, and thus to refractive index modulation. It will be this refractive index modulation which induces the beam coupling which we seek to describe.

The electric field inside the cell bulk is given by taking the gradient of Eq. (12). We find

$$E_x(x,z) = E_{1q}(z)\cos qx + E_{2q}(z)\sin qx,$$

$$E_z(x,z) = E_0 + E_z',$$

$$E_z'(x,z) = E_{3q}(z)\cos qx + E_{4q}(z)\sin qx, \tag{13}$$

where

$$E_0 = -\frac{\Phi_0}{L}, \tag{14}$$

$$E_{1q} = q\Phi_1 \frac{\sin\delta}{\sinh\tilde{q}L}\sinh\tilde{q}z, \tag{15}$$

$$E_{2q} = q\Phi_1\left(\cosh\tilde{q}z + \frac{\cos\delta - \cosh\tilde{q}L}{\sinh\tilde{q}L}\sinh\tilde{q}z\right), \tag{16}$$

$$E_{3q} = -\tilde{q}\Phi_1\left(\sinh\tilde{q}z + \frac{\cos\delta - \cosh\tilde{q}L}{\sinh\tilde{q}L}\cosh\tilde{q}z\right), \tag{17}$$

$$E_{4q} = \tilde{q}\Phi_1 \frac{\sin\delta}{\sinh\tilde{q}L}\cosh\tilde{q}z. \tag{18}$$

It will be useful later to normalize the field E_{iq} with respect to the externally imposed field

$$e_{iq}(z) = \frac{E_{iq}}{E_0} = a_i\cosh\tilde{q}z + b_i\sinh\tilde{q}z, \tag{19}$$

where the quantities a_i, b_i are given by

i	a_i	b_i
1	0	$-qL\frac{\Phi_1}{\Phi_0}\frac{\sin\delta}{\sinh\tilde{q}L}$
2	$-qL\frac{\Phi_1}{\Phi_0}$	$-qL\frac{\Phi_1}{\Phi_0}\frac{\cos\delta-\cosh\tilde{q}L}{\sinh\tilde{q}L}$
3	$\tilde{q}L\frac{\Phi_1}{\Phi_0}\frac{\cos\delta-\cosh\tilde{q}L}{\sinh\tilde{q}L}$	$\tilde{q}L\frac{\Phi_1}{\Phi_0}$
4	$\tilde{q}L\frac{\Phi_1}{\Phi_0}\frac{\sin\delta}{\sinh\tilde{q}L}$	0

III. DIRECTOR PROFILE IN THE LIQUID CRYSTAL CELL

We now determine the director profile in the liquid crystal cell in the presence of the electric fields given by Eq. (13). The bulk free energy F_V of a distorted nematic liquid crystal in an applied electric field takes the form

$$F_V = \frac{1}{2}K_{11}\int(\boldsymbol{\nabla}\cdot\mathbf{n})^2 dV + \frac{1}{2}K_{22}\int(\mathbf{n}\cdot\boldsymbol{\nabla}\times\mathbf{n})^2 dV + \frac{1}{2}K_{33}\int(\mathbf{n}\times\boldsymbol{\nabla}\times\mathbf{n})^2 dV - \frac{1}{2}\int\mathbf{D}\cdot\mathbf{E}\cdot\mathbf{d}\cdot\mathbf{V} \tag{20}$$

with the electric displacement $\mathbf{D}=\hat{\varepsilon}\mathbf{E}$, $\varepsilon_{ij}=\varepsilon_\perp\delta_{ij}+\varepsilon_a n_i n_j$, with the anisotropic part of the static dielectric constant $\varepsilon_a=\varepsilon_\parallel-\varepsilon_\perp$.

The electric field felt by the liquid crystal molecules has a number of contributions. The first is the externally imposed voltage. The second is the periodic modulation in the x direction discussed in the last section. This is an indirect effect of the light field acting on the surface layer, transmitted into the bulk as a result of the effect of the Laplace equation. A final contribution comes from the direct effect of the light field on the liquid crystal. We are assuming here that this can be neglected. The justification for this is empirical, and derives from the observation that in the absence of the surface layers, the effect essentially disappears [8,24]. The director field is now given by $n=[\sin\theta(x,z),0,\cos\theta(x,z)]$, with θ small.

The variational problem to be solved consists of minimizing Eq. (20), subject to strong anchoring homeotropic boundary conditions $\theta(x,z=0)=\theta(x,z=L)=0$ at each wall, and subject also to the electric fields given in Eq. (13). We simplify further by supposing the so-called one constant approximation, i.e., the splay and bend Frank-Oseen elastic coefficients are equal: $K_{11}=K_{33}=K$.

The relevant part of the thermodynamic functional (20) is now given by

$$F = \frac{1}{2}\int\int\{K[(\theta_x')^2+(\theta_z')^2] - \varepsilon_a[(E_x^2-E_z^2)\sin^2\theta + E_xE_z\sin 2\theta]\}dxdz. \tag{21}$$

The Euler-Lagrange equation for this functional is

$$K\left(\frac{\partial^2\theta}{\partial x^2}+\frac{\partial^2\theta}{\partial z^2}\right) + \varepsilon_a[(E_x^2-E_z^2)\sin\theta\cos\theta + E_xE_z\cos 2\theta] = 0. \tag{22}$$

We solve Eq. (22) in the limit $\frac{E_x}{E_0}\ll 1$, $\frac{E_z'}{E_0}\ll 1$. This corresponds, roughly speaking, to high voltage or low beam intensities. The resulting solution may also be qualitatively valid if $\frac{E_x}{E_0}\leqslant 1$, $\frac{E_z'}{E_0}\leqslant 1$. Expanding to linear order in θ and $\frac{E_x}{E_0}$ we obtain

$$\xi^2\left(\frac{\partial^2\theta}{\partial x^2}+\frac{\partial^2\theta}{\partial z^2}\right) = \theta - \frac{E_x}{E_0}, \tag{23}$$

where the length scale ξ is the relaxation length set by the bulk electric field, with $\xi^{-2}=\frac{\varepsilon_a E_0^2}{K}$. In order to do this, we linearize Eq. (23) for components $\theta_{1q}=\vartheta_1(z)\cos qx$ and $\theta_{2q}=\vartheta_2(z)\sin qx$ of the director reorientation of wave number q in the cell plane.

It is convenient at this stage to reformulate the problem in terms of nondimensional variables. We define a rescaled

length along the cell $\rho=\frac{z}{L}$, $\rho\in[0,1]$, a rescaled transverse wave vector $\mu=\tilde{q}L$, and a rescaled voltage $\nu=\frac{L}{\xi}=LE_0(\frac{\varepsilon_a}{K})^{1/2}$. For some purposes it is convenient to measure length not from the plane of incidence, but rather from the midplane of the cell. We can define a length variable $\sigma=\rho-1/2$, and then inside the cell $\sigma\in[-1/2,1/2]$.

Equation (23) now reduces to

$$\frac{d^2\vartheta_i(\rho)}{d\rho^2}-\kappa^2\vartheta_i(\rho)=-\nu^2 e_{iq}(\rho) \tag{24}$$

with $\kappa^2=\mu^2+\nu^2$.

This equation can be solved using standard methods and has the solution

$$\theta(x,z)=-qL\frac{\Phi_1}{\Phi_0}\Bigg(\cos qx\sin\delta\left[\frac{\sinh\mu\rho}{\sinh\mu}-\frac{\sinh\kappa\rho}{\sinh\kappa}\right]+\sin qx\Bigg[\cosh\mu\rho-\cosh\kappa\rho+\frac{\cos\delta-\cosh\mu}{\sinh\mu}\sinh\mu\rho+\frac{\cosh\kappa-\cos\delta}{\sinh\kappa}\sinh\kappa\rho\Bigg]\Bigg). \tag{25}$$

For some purposes it is more convenient to rewrite Eq. (26) as

$$\theta(x,z)=-qL\frac{\Phi_1}{\Phi_0}\Bigg(\cos\frac{\delta}{2}\sin\left(qx+\frac{\delta}{2}\right)\left\{\frac{\cosh\mu\sigma}{\cosh\mu/2}-\frac{\cosh\kappa\sigma}{\cosh\kappa/2}\right\}+\sin\frac{\delta}{2}\cos\left(qx+\frac{\delta}{2}\right)\left\{\frac{\sinh\mu\sigma}{\sinh\mu/2}-\frac{\sinh\kappa\sigma}{\sinh\kappa/2}\right\}\Bigg). \tag{26}$$

The advantage of the expression (26) is that the variation of $\theta(x,z)$ is expressed in terms of components that are respectively out-of-phase and in-phase with the total optical field intensities on the midplane. This expression explicitly exhibits the symmetry of the system around the midplane.

We discuss in the next section in detail how to use $\theta(x,z)$ to calculate nonlinear optical effects. However, we note that in general the larger the values of $\theta(x,z)$ measured in some sense the larger will be the optical effect. It is therefore of some interest to monitor the behavior of $\theta(x,z)$ as a function of system parameters.

We plot the z dependence of the out-of-phase component of $\theta(x,z)$ in Fig. 2. One might expect a roughly sinusoidal dependence, with a maximum at the cell midplane. And indeed, for closely matched incident beams, with a low wave-number interference pattern, this is what occurs. But when the nondimensional grating wave vector μ is larger than unity, the sinusoidal dependence no longer holds. By $\mu=4$, the response is flattened, and by $\mu\sim6$ the profile has developed a double hump structure. Not only is the shape unexpected, but the magnitude is reduced in this regime, and as discussed in the last paragraph, this should (and, as we shall see below, does) lead to a reduced non-linear optical effects for larger μ.

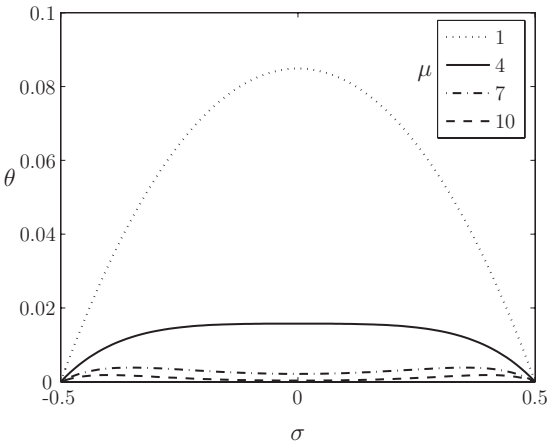

FIG. 2. Functional dependence of angular distortion from homeotropic texture, in the limit of low field, for different values of the nondimensionalized grating wave number μ. This figure shows the component of the angular distortion out-of-phase with the intensity modulations.

From Eq. (26) we observe that $\Theta=(\frac{1}{\cosh(\mu/2)}-\frac{1}{\cosh(k/2)})$ can be regarded as a figure of merit for the degree of distortion of the liquid crystal. This is a measure of the amplitude of the response at the midplane of the cell. We note that Θ technically only measures the out-of-phase distortion, and furthermore even then the magnitude of the distortion is not maximal at the midplane of the cell. Nevertheless it serves in a rough and ready way as a surrogate for the magnitude of the grating response to optical probes. In Fig. 3 we plot Θ as a function of voltage.

IV. DIFFRACTION OF LIGHT BEAMS

A. Formulation of problem

We now consider light beam propagation of each of the two waves through the (now) weakly nonuniform anisotropic liquid crystal cell. We suppose the wave incident from the vacuum to have wave number $\mathbf{k}=k\hat{\mathbf{k}}$, with $k=2\pi/\lambda=\omega/c$,

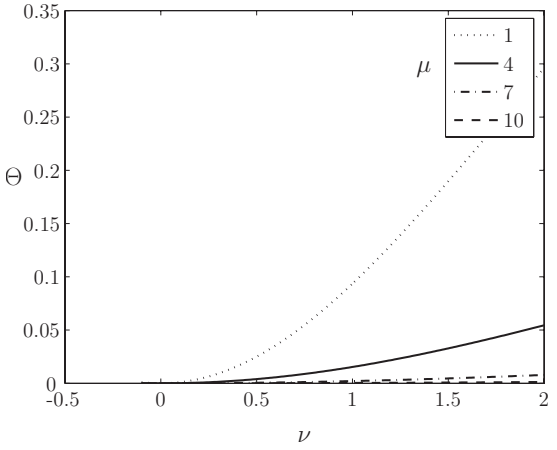

FIG. 3. Dependence of the amplitude of the component of the angular distortion out-of-phase with the optical intensity, as a function of nondimensionalized voltage

where the angular frequency ω and the speed of light c take their usual meanings. In the presence of a uniform liquid crystal, the light will be refracted into an ordinary (o) and an extraordinary (e) wave. The ordinary wave is polarized perpendicularly to the plane of incidence (in the y direction) and the refractive index which corresponds to this wave is $n_o = \sqrt{\varepsilon_\perp}$. For the extraordinary wave the effective refractive index is given by

$$n_{\text{eff}}(\psi) = \frac{\sqrt{\varepsilon_\parallel \varepsilon_\perp}}{\sqrt{\varepsilon_\parallel \cos^2\psi + \varepsilon_\perp \sin^2\psi}}, \tag{27}$$

where ψ is the angle between the director and the direction of propagation inside the medium.

The effect of the nonuniformity will be to modulate the amplitude of the wave in the plane of the outgoing surface, and hence in addition to the refraction, diffraction will also occur. The purpose of this section is to calculate the magnitude of this diffraction. There are in fact two waves, but first we discuss the effect of the modified director on each individual wave.

B. The dielectric function

The dielectric function is given by

$$\varepsilon_{ij} = \varepsilon_\perp \delta_{ij} + \varepsilon_a n_i n_j, \tag{28}$$

with $\varepsilon_a = \varepsilon_\parallel - \varepsilon_\perp$ and director components n_i. In the limit of interest in this paper, the director deviations from the initial homeotropic alignment are small. Then

$$n = [\sin\theta(x,z), 0, \cos\theta(x,z)] \approx [\theta(x,z), 0, 1]. \tag{29}$$

The dielectric function now simplifies to

$$\hat{\varepsilon} = \hat{\varepsilon}_0 + \theta(x,z)\hat{\varepsilon}_1 \tag{30}$$

or, alternatively,

$$\hat{\varepsilon} = \begin{pmatrix} \varepsilon_\perp & 0 & 0 \\ 0 & \varepsilon_\perp & 0 \\ 0 & 0 & \varepsilon_\parallel \end{pmatrix} + \theta(x,z) \begin{pmatrix} 0 & 0 & \varepsilon_a \\ 0 & 0 & 0 \\ \varepsilon_a & 0 & 0 \end{pmatrix}. \tag{31}$$

C. Geometrical optics

The theoretical strategy involves determining perturbations around the transmission through the pure homeotropic (i.e., $\hat{\varepsilon}_0$) system. The characteristic length for director inhomogeneity in the z direction is the cell thickness L. In the x direction the corresponding characteristic length is the grating period $\Lambda = 2\pi/q$. We shall use the geometrical optics approximation (GOA) [25–27], valid in the limits $\lambda \ll L$ and $\lambda \ll \Lambda$.

We seek solutions to the Maxwell equations

$$\nabla \times \mathbf{E} = -\mu \frac{\partial \mathbf{H}}{\partial t}, \quad \nabla \times \mathbf{H} = \frac{\partial}{\partial t} \varepsilon_0 \hat{\varepsilon} \mathbf{E} \tag{32}$$

in the following forms:

$$\mathbf{E}(\mathbf{r},t) = \exp[-i\omega t + ikS(\mathbf{r})]\mathbf{E}_0,$$

$$\mathbf{H}(\mathbf{r},t) = \exp[-i\omega t + ikS(\mathbf{r})]\mathbf{H}_0. \tag{33}$$

The term $S(\mathbf{r})$ is the optical path length or "eikonal," and the local direction of the wave vector is given by $\nabla S(\mathbf{r})$.

Substituting Eqs. (33) into the Maxwell equations (32), we obtain the following pair of equations:

$$k\,\nabla S(\mathbf{r}) \times \mathbf{E}_0 = \mu_0 \omega \mathbf{H}_0; \quad k\,\nabla S(\mathbf{r}) \times \mathbf{H}_0 = -\varepsilon_0 \hat{\varepsilon} \omega \mathbf{E}_0. \tag{34}$$

The magnetic field $\mathbf{H}_0$ can now be eliminated, yielding a homogeneous equation for $\mathbf{E}_0$:

$$\nabla S(\mathbf{r}) \times [\nabla S(\mathbf{r}) \times \mathbf{E}_0] + \hat{\varepsilon}\mathbf{E}_0 = 0. \tag{35}$$

Equation (35) is a homogeneous system of linear equations for the electric field components, analogous to a vector Helmholtz equation. In general solutions to this equation will be trivial and uninteresting. However, there are non-trivial solutions, corresponding to optical traveling waves, if the determinant of this set of equations is null.

In fact the determinant factorizes. An E eigenvector in the y direction corresponds to the ordinary wave. The perturbations in the dielectric tensor do not affect transmission of the ordinary wave through the sample, and we shall not be interested in this mode of transmission. The E eigenvector in the x-z plane (i.e., the plane of incidence) corresponds to the extraordinary (e) wave. The pair of homogeneous equations are

$$\begin{bmatrix} \varepsilon_\perp - (\partial_z S)^2 & \partial_x S \partial_z S + \varepsilon_a \theta(x,z) \\ \partial_x S \partial_z S + \varepsilon_a \theta(x,z) & \varepsilon_\parallel - (\partial_x S)^2 \end{bmatrix} \begin{bmatrix} E_x \\ E_z \end{bmatrix} = 0. \tag{36}$$

The null determinant condition appropriate to the e-wave now reduces to [35]

$$[\varepsilon_\perp - (\partial_z S)^2][\varepsilon_\parallel - (\partial_x S)^2] - [\partial_x S \partial_z S + \varepsilon_a \theta(x,z)]^2 = 0. \tag{37}$$

D. Perturbation theory

In the absence of the director modulation, the e-wave is directly transmitted. We consider Eq. (37) as a perturbation of this process. We therefore recast Eq. (37) to lowest order in $\theta(x,z)$:

$$\frac{(\partial_x S)^2}{\varepsilon_\parallel} + \frac{(\partial_z S)^2}{\varepsilon_\perp} + 2\left(\frac{\varepsilon_a}{\varepsilon_\parallel \varepsilon_\perp}\right)(\partial_x S \partial_z S)\,\theta(x,z) = 1. \tag{38}$$

In the spirit of the WKB approximation, the solution of Eq. (38) can be expressed as the sum of an unperturbed e wave, plus a small phase change $f(\mathbf{r})$ which can be ascribed solely to the modulation. Thus,

$$S(r) = S_0(r) + f(\mathbf{r}), \tag{39}$$

where S_0 obeys the equation

$$\frac{(\partial_x S_0)^2}{\varepsilon_\parallel} + \frac{(\partial_z S_0)^2}{\varepsilon_\perp} = 1. \tag{40}$$

We note also that the effective refractive index n_{eff} can be defined as

$$(\nabla S_0)^2 = n_{\text{eff}}^2. \tag{41}$$

Combining Eqs. (40) and (41) yields the well-known expression for the refractive index (27). The wave vector inside the medium is now given by

$$\mathbf{k}' = k\,\nabla S_0 = k[\partial_x S_0, 0, \partial_z S_0] = k'[\sin\psi, 0, \cos\psi], \tag{42}$$

with $k' = kn_{\text{eff}}$.

Combining Eqs. (38)–(40), we can obtain the leading order equation for the phase $f(x,z)$:

$$(\partial_x S_0)\frac{\partial_x f}{\varepsilon_\parallel} + (\partial_z S_0)\frac{\partial_z f}{\varepsilon_\perp} = -(\partial_x S_0)(\partial_z S_0)\frac{\varepsilon_a \theta(x,z)}{\varepsilon_\parallel \varepsilon_\perp}. \tag{43}$$

We now substitute Eq. (42) into Eq. (43), yielding

$$\left(\frac{\sin\psi}{\varepsilon_\parallel}\right)\frac{\partial f}{\partial x} + \left(\frac{\cos\psi}{\varepsilon_\perp}\right)\frac{\partial f}{\partial z} = -\sin\psi\cos\psi\left(\frac{\varepsilon_a n_{\text{eff}}}{\varepsilon_\parallel \varepsilon_\perp}\right)\theta(x,z). \tag{44}$$

Equation (44) can be solved using the method of characteristics. The left-hand side of this equation can be transformed into a total derivative

$$\begin{aligned}\frac{df}{dz} &= \frac{\partial f}{\partial z} + \left(\frac{dx}{dz}\right)\left(\frac{\partial f}{\partial x}\right) \\ &= \frac{\partial f}{\partial z} + \left(\frac{\varepsilon_\perp \sin\psi}{\varepsilon_\parallel \cos\psi}\right)\left(\frac{\partial f}{\partial x}\right) \\ &= \frac{\partial f}{\partial z} + \tan\psi'\left(\frac{\partial f}{\partial x}\right).\end{aligned} \tag{45}$$

Combining Eqs. (44) and (45) yields

$$\frac{df}{dz} = -\sin\psi\left(\frac{\varepsilon_a}{\varepsilon_\parallel}\right)n_{\text{eff}}\theta(x,z), \tag{46}$$

where now the quantities x and z in this equation are explicitly related by

$$\frac{dx}{dz} = \tan\psi', \tag{47}$$

defined in Eq. (45). Equation (47) allows a family of solutions

$$x(z,x_0) = x_0 + z\tan\psi'. \tag{48}$$

We note that each member of this family of solutions represents a wave entering the liquid crystal sample at position x_0. The direction of wave propagation is given by the angle ψ. However, because this medium is anisotropic, the angle of the energy propagation, given by the Poynting vector, is determined by the angle ψ'. The family of solutions $x(z,x_0)$ corresponds to paths in the undistorted anisotropic medium with different x_0 traveling in the direction of the Poynting vector.

Now we can solve Eq. (46) directly, by integrating the right-hand side, yielding

$$f(x,z) = -\sin\psi\left(\frac{\varepsilon_a n_{\text{eff}}}{\varepsilon_\parallel}\right)\int_0^z \theta[x'(z',x_0),z']dz', \tag{49}$$

where the integration path is such that $x = x_0 + z\tan\psi'$, $x' = x_0 + z'\tan\psi'$ and, hence,

$$x' = x - (z - z')\tan\psi'. \tag{50}$$

Thus

$$f(x,z) = -\sin\psi\left(\frac{\varepsilon_a n_{\text{eff}}}{\varepsilon_\parallel}\right)\int_0^z \theta[x - (z-z')\tan\psi', z']dz', \tag{51}$$

The key quantity of interest is the phase retardation of the beam as it leaves the cell, i.e., at $z=L$. We now rewrite Eq. (49), so as to express this quantity directly

$$f(x,L) = -\sin\psi\left(\frac{\varepsilon_a n_{\text{eff}}}{\varepsilon_\parallel}\right)\int_0^L \theta[x - (L-z')\tan\psi', z']dz' \tag{52}$$

E. Diffraction pattern

The formula (52) applies to all incident light beams. We confine our interest to the cases in which there are two incident beams, with wave numbers k_1 and k_2, with $k_{1x} - k_{2x} = q$. Equation (52) permits the calculation the light fields of the beams as they exit the liquid crystal cell. By suitably decomposing these light field into Fourier components, it is possible to identify the amplitudes of particular diffracted beams.

The light field along the plane $z=L$ is modulated by the factor

$$\begin{aligned}\exp[ikS(x,L)] &= \exp\{i[\mathbf{k}'\cdot\mathbf{r} + kf(\mathbf{r})]\} \\ &= \exp\{i[k_x x + k_z' L + kf(x,L)]\} \\ &= \exp[i(k_x x + \delta\phi_0 + \delta\phi_1)],\end{aligned} \tag{53}$$

where $\delta\phi_0 = k_z' L = kn_{\text{eff}} L\cos\psi$, and $\delta\phi_1 = kf(x,L)$;

$$\delta\phi_0 = \frac{\sqrt{\varepsilon_\parallel \varepsilon_\perp}}{(\varepsilon_\parallel \cos^2\psi + \varepsilon_\perp \sin^2\psi)^{1/2}}(kL\cos\psi) \tag{54}$$

and

$$\delta\phi_1 = -k\frac{\sqrt{\varepsilon_\perp}(\varepsilon_\parallel - \varepsilon_\perp)\sin\psi}{\sqrt{\varepsilon_\parallel}(\varepsilon_\parallel\cos^2\psi + \varepsilon_\perp\sin^2\psi)^{1/2}} \times\left[\int_0^L \theta[x - (L-z')\tan\psi', z']dz'\right]. \tag{55}$$

The quantity $\delta\phi_1(x)$ is the varying component of the additional phase of the incident beam, following from the director modulation in the liquid crystal medium. We now recall that from Eq. (26) the director profile can be written in a sinusoidal form $\theta(x,z) \propto \cos(qx+\Delta)$. Combining this result with Eq. (55) yields the result

$$\delta\phi_1(x) = B\cos(qx + \tilde{\Delta}), \tag{56}$$

where the phase modulation parameters $B>0$ and $\tilde{\Delta}$ are, respectively, the amplitude and phase of the additional phase $\delta\phi_1(x)$:

$$B = \sqrt{A^2 + C^2}, \quad \tan\tilde{\Delta} = -\frac{A}{C}. \tag{57}$$

After complicated but straightforward algebra using Eqs. (26) and (55), expressions for the quantities A and C can be derived:

$$A = -kL\frac{\Phi_1}{\Phi_0}\frac{\mu(\varepsilon_\parallel - \varepsilon_\perp)\sin\psi}{(\varepsilon_\parallel\cos^2\psi + \varepsilon_\perp\sin^2\psi)^{1/2}}\int_{-1/2}^{1/2}\left(\cos\frac{\delta}{2}\left\{\frac{\cosh\mu\sigma}{\cosh\mu/2} - \frac{\cosh\kappa\sigma}{\cosh\kappa/2}\right\}\cos\left[\mu\left(\sigma - \frac{1}{2}\right)\tan\psi'\right] - \sin\frac{\delta}{2}\left\{\frac{\sinh\mu\sigma}{\sinh\mu/2} - \frac{\sinh\kappa\sigma}{\sinh\kappa/2}\right\}\sin\left[\mu\left(\sigma - \frac{1}{2}\right)\tan\psi'\right]\right)d\sigma, \tag{58}$$

$$C = -kL\frac{\Phi_1}{\Phi_0}\frac{\mu(\varepsilon_\parallel - \varepsilon_\perp)\sin\psi}{(\varepsilon_\parallel\cos^2\psi + \varepsilon_\perp\sin^2\psi)^{1/2}}\int_{-1/2}^{1/2}\left(\cos\frac{\delta}{2}\left\{\frac{\cosh\mu\sigma}{\cosh\mu/2} - \frac{\cosh\kappa\sigma}{\cosh\kappa/2}\right\}\sin\left[\mu\left(\sigma - \frac{1}{2}\right)\tan\psi'\right] + \sin\frac{\delta}{2}\left\{\frac{\sinh\mu\sigma}{\sinh\mu/2} - \frac{\sinh\kappa\sigma}{\sinh\kappa/2}\right\}\cos\left[\mu\left(\sigma - \frac{1}{2}\right)\tan\psi'\right]\right)d\sigma. \tag{59}$$

Now Eq. (53) can be rewritten, using Eq. (56), so as explicitly identify different components of the diffracted wave. The key relation is the Jacobi-Anger expansion [28]

$$\exp(iz\cos\phi) = \sum_{n=-\infty}^{n=+\infty}(i)^n J_n(z)\exp(in\phi). \tag{60}$$

Combining Eq. (60) with Eqs. (53)–(56) yields the expansion for the electric field at the output surface

$$\begin{aligned} E_{\text{out}} &= E_0\exp(i\delta\phi_0 + ik_x x)\exp(i\delta\phi_1) \\ &= E_0\exp(i\delta\phi_0 + ik_x x)\sum_{n=-\infty}^{\infty}(i)^n J_n(B)\exp(inqx + in\tilde{\Delta}). \end{aligned} \tag{61}$$

Now we can identify [29] terms in this expansion with the amplitudes $X^{(n)}$ and phases $\delta^{(n)}$ of outgoing waves in the diffraction pattern

$$X^{(n)} = (i)^n J_n(B) \tag{62}$$

and

$$\delta^{(n)} = \delta\phi_0 + n\tilde{\Delta}. \tag{63}$$

The electric field in the diffracted wave of order n then takes the form

$$\frac{E_n}{E_0} = X^{(n)}\exp i(\mathbf{k}^{(n)}\cdot\mathbf{r} + \delta^{(n)}), \tag{64}$$

where $\mathbf{k}^{(n)}$ is the wave number of the diffracted wave of order n, with $k_x^{(n)} = k_x + nq$, and $|\mathbf{k}^{(n)}| = |\mathbf{k}|$.

F. Beam coupling

We now return to the original problem (5) in which there are two incident waves with wave numbers $\mathbf{k}_1$, $\mathbf{k}_2$, and with $k_{1x} - k_{2x} = q$. Beam coupling corresponds the diffraction of waves from incident wave $\mathbf{k}_1$ to outgoing wave $\mathbf{k}_2 = \mathbf{k}_1 - q\mathbf{e}_x$, and from incident wave $\mathbf{k}_2$ to outgoing wave $\mathbf{k}_1 = \mathbf{k}_2 + q\mathbf{e}_x$. Thus the diffracted wave of order -1 from $\mathbf{k}_1$ adds coherently with the directly transmitted wave $\mathbf{k}_2$, and the diffracted wave of order $+1$ from $\mathbf{k}_2$ adds coherently with the directly transmitted wave $\mathbf{k}_1$. Equivalently, using the notation of the last section $\mathbf{k}_1 = \mathbf{k}_2^{(+1)}$ and $\mathbf{k}_2 = \mathbf{k}_1^{(-1)}$.

We are thus able to use terms from the diffraction expression (64) to evaluate the amplitudes of the outgoing waves directions $\mathbf{k}_1$ and $\mathbf{k}_2$. We find

$$\begin{aligned} E_{\text{out}}(\mathbf{k}_1) &= E_{01}X^{(0)}\exp(i\delta^{(0)}) + E_{02}X^{(+1)}\exp(i\delta^{(+1)}), \\ E_{\text{out}}(\mathbf{k}_2) &= E_{01}X^{(-1)}\exp(i\delta^{(-1)}) + E_{02}X^{(0)}\exp(i\delta^{(0)}). \end{aligned} \tag{65}$$

We note that in principle the quantities $X^{(n)}$ depend on the value of the incident wave number. However, in the two-beam coupling case discussed here, the incident waves have wave numbers very nearly equal to each other, and so we may consider the quantities $X^{(n)}$ to be the same for each incident wave.

From Eq. (66), we can evaluate the outgoing wave intensities, using the relation $I = \mathbf{E}\cdot\mathbf{E}^*$. Using Eq. (63). We find

$$\begin{aligned} I_{\text{out}}(\mathbf{k}_1) = [&E_{01}\exp(i\delta^{(0)})J_0(B) + iE_{02}\exp(i\delta^{(+1)})J_1(B)] \\ &\times\{[E_{01}^*\exp(-i\delta^{(0)})J_0(B) \\ &- iE_{02}^*\exp(-i\delta^{(+1)})J_1(B)]\}, \end{aligned} \tag{66}$$

or

$$I_{\text{out}}(\mathbf{k}_1) = I_1 J_0^2(B) + I_2 J_1^2(B) - 2\sqrt{I_1 I_2} J_0(B) J_1(B) \sin(\tilde{\Delta}),$$

$$I_{\text{out}}(\mathbf{k}_2) = I_2 J_0^2(B) + I_1 J_1^2(B) + 2\sqrt{I_1 I_2} J_0(B) J_1(B) \sin(\tilde{\Delta}), \tag{67}$$

where $\tilde{\Delta}$ is as defined in Eq. (57).

It is usual to consider one of the beams as the *pump* beam and the other as the probe beam. Without loss of generality, we shall suppose that $\mathbf{k}_1$ corresponds to the pump beam and $\mathbf{k}_2$ to the probe beam. In line with the literature, we define

$$m = \frac{I_{\text{probe}}}{I_{\text{pump}}} = \frac{I_2}{I_1}. \tag{68}$$

We can now rewrite the formulas for the outgoing beam intensities in terms of the quantity m as follows:

$$I_{\text{out}}(\mathbf{k}_1) = I_1[J_0^2(B) + mJ_1^2(B) - 2\sqrt{m} J_0(B) J_1(B) \sin(\tilde{\Delta})],$$

$$I_{\text{out}}(\mathbf{k}_2) = I_1[mJ_0^2(B) + J_1^2(B) + 2\sqrt{m} J_0(B) J_1(B) \sin(\tilde{\Delta})]. \tag{69}$$

The degree of beam coupling can now be characterized by the gain g. This is the ratio of the intensity of the outgoing beam in the direction of the probe beam in the presence of the pump beam to the intensity of the same beam in the absence of the pump beam. In the context of this paper, in which we do not consider reflection and refraction at the cell walls, the quantity g is defined as

$$g = \frac{I_{\text{out}}(\mathbf{k}_2)}{I_2} = J_0^2(B) + \frac{1}{m} J_1^2(B) + 2\frac{1}{\sqrt{m}} J_0(B) J_1(B) \sin(\tilde{\Delta}). \tag{70}$$

A related quantity is the diffraction efficiency η, which measures the strength with which the grating diffracts the probe beam. The formal definition is the ratio of the intensity of the diffracted probe beam (i.e. in the direction of the pump beam) to that of the incoming probe beam. From Eqs. (62) and (64), this is

$$\eta = |X^{(-1)}|^2 = J_1^2(B). \tag{71}$$

For ease of presentation of our results, it is also convenient to define quantities η' and g'. These quantities are, respectively, analogous to η and g, but with the roles of the pump and probe beams exchanged.

V. RESULTS

A. Analytical study of the behavior of intensities

First we discuss diffraction from a single beam. The transmitted energy is divided between beams of different orders n. The amplitude of diffracted beams is given by $|X^{(n)}|^2 \propto J_n^2(B)$ [Eq. (63)], where we recall, from Eq. (57) that B is the amplitude of the additional phase variations induced by the spatial modulations in the liquid crystal layer. We introduce the energy conservation parameter

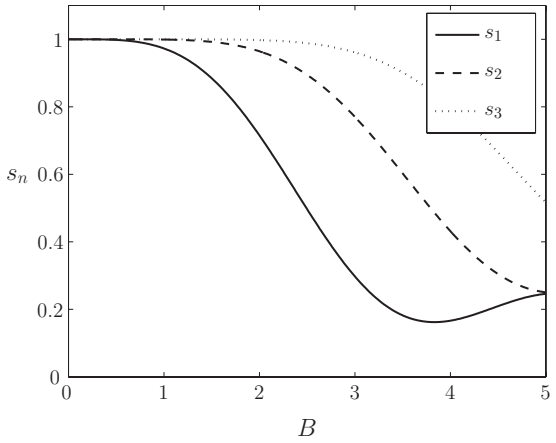

FIG. 4. The dependence of energy conservation parameter $s_n(B)$ on phase modulation parameter B. Solid line: s_1, dashed line: s_2, and dotted line: s_3. See text for further discussion.

$$s_n(B) = \sum_{k=-n}^{k=n} J_k^2(B). \tag{72}$$

The quantity $s_n(B)$ describes the proportion of transmitted energy that is distributed between diffracted beams of orders from $-n$ to n. We note that in the limit $n \to \infty$ necessarily $s_n \to 1$.

In Fig. 4 we show the dependence of s_n on the phase modulation parameter B for low n. For small B ($B \leqslant 1$), $s_1(B) \approx 1$. In this regime almost all transmitted energy is either in the directly transmitted beam, or in the first-order diffracted beam. This is the regime in which energy exchange between two beams is most effective.

As B increases, an increasing proportion of the transmitted energy is transferred to outlying diffracted beams. The quantity s_2 remains essentially unity until $B \approx 1.5$, while s_3 only noticeably departs from unity at $B \approx 2.5$. We shall return to the problem of the asymptotic behavior of $s_n(B)$ for large n, B elsewhere. For this study, however, we shall be interested in the small B regime.

We now analyze the effect of energy exchange in the presence of both incident beams. We shall take equal intensities in Eq. (69) for incident beams $m=1$. In principle, the parameter m [Eq. (68)], measuring the ratio of the intensities of the beams, can take any value. In our calculations we shall suppose $m=1$; this corresponds to equal intensity beams. This will enable us to make contact with previous studies [2], which have also used this value. In addition it is easy to monitor energy transfer between beams. We note that in devices we may well expect that $m \ll 1$, so that a large reservoir of pump beam energy is available to amplify a given probe beam.

The degree of energy transfer is critically dependent on the quantity $\tilde{\Delta}$, defined in Eq. (57). When $\tilde{\Delta}=0$, the modulation of the phase retardation is in-phase with the intensity modulation due to the beam interference. If $m=1$, Eq. (69) implies that there is no net energy exchange between the beams. This is consistent with general intuition [30] that a phase difference between the intensity and dielectric modu-

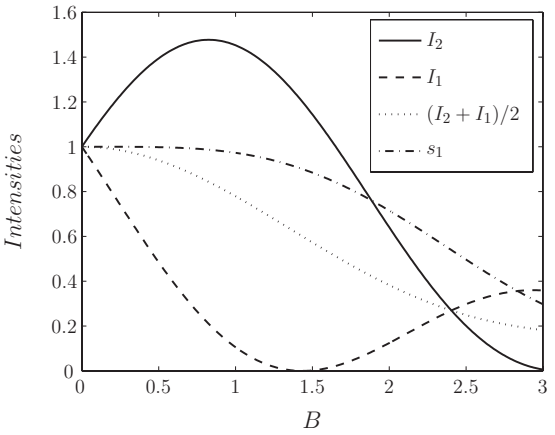

FIG. 5. The behavior of functions $I_2(B)$ (solid curve) and $I_1(B)$ (dot curve) when $\sin(\tilde{\Delta})=1$.

lations is required for beam coupling. Interestingly, although we do not pursue this here, this rule no longer holds for the $m\neq 1$ case.

The maximum energy transfer between beams occurs when $\sin(\tilde{\Delta})=1$. In this case the two outgoing beams obey the following rule:

$$I_1 \propto [J_0(B)-J_1(B)]^2,$$

$$I_2 \propto [J_0(B)+J_1(B)]^2. \tag{73}$$

The behavior of these functions is shown in Fig. 5. The function $I_2(B)$ (solid curve on the graph) reaches a maximum value of ≈ 1.48 at $B\approx 0.85$. We also plot $I_1(B)$, and note that this reaches a minimum (at zero) for $B\approx 1.4$. The quantity

$$\bar{I}(B)=\frac{1}{2}[I_1(B)+I_2(B)] \tag{74}$$

denotes that proportion of the energy of the incident beams which remains in the two initial beams directions. The quantity $\bar{I}(B)$ is unity for $B=0$ (at which there is, however, no energy exchange) and reduces steadily with B. Close to the maximum $I_2(B)\approx 1.48$ at $B\approx 0.85$, $\bar{I}(B)\approx 0.8$, reducing monotonically to $\bar{I}(B\approx 2)\approx 0.4$. However, for $B\leqslant 1$, $s_1(B)$ is essentially unity. The energy lost from the primary beams reappears as other $|n|=1$ diffracted beams. Subsequent maxima of $I_2(B)$ take values less than unity, in regimes in which a substantial proportion of the transmitted energy is lost in outlying diffracted beams. Thus the appearance of energy transfer between beams is restricted to the first maximum of $I_2(B)$.

B. Dependence on external parameters

We now examine quantitatively the energy exchange process, using experimentally plausible parameters. A list of parameters in the problem is given in Table I, together with meanings of these parameters, and where appropriate, the numerical values that we have used in our calculations.

The final element in the theory enabling comparison with experiment is the response of the surface potential Φ_1 to the local beam intensity. We do not, however, have a microscopic photoelectrochemical theory to describe this process. In principle, Φ_1 is a measurable quantity, although in practice the measurement may be difficult to carry out.

TABLE I. Table of parameters.

Parameter	Value	Description
λ	0.63 μm	Wavelength of incident beams
L	20 μm	Thickness of the film
$\varepsilon_\perp$, $\varepsilon_\parallel$	1.5^2, 1.7^2	Dielectric permittivities of the liquid crystal
ψ	variable	Angle of propagation inside liquid crystal
δ	variable	Phase shift between the interference patterns at top and bottom surfaces. This is the surrogate for the angle of incidence which we do not include explicitly
γ	variable	Half angle between beams defining the dimensionless grating wave vector $\mu=\tilde{q}L=2kL\sqrt{\frac{\varepsilon_\perp}{\varepsilon_\parallel}}\cos\psi\sin\gamma$
μ	variable	Nondimensional grating wave vector $\mu=\tilde{q}L$ for $\gamma\approx 2.4^\circ$, $\mu\approx 6$.
ν	1	Dimensionless voltage $\nu=LE_0(\frac{\varepsilon_a}{K})^{1/2}$
m	1	Ratio of intensities of incoming beams

In our initial calculations we suppose $\Phi_1/\Phi_0=1$ [Eq. (26)] and the external voltage $\nu=1$. We first investigate the dependence of energy exchange effect on ψ. We set the grating period $\mu=6$, which corresponds to a grating wavelength Λ equal to the cell thickness L.

The key intermediate parameters governing g [Eq. (70)] and η [Eq. (71)] are the phase modulation parameters B and $\tilde{\Delta}$. In Fig. 6 we plot the phase modulation parameter B as a function of ψ, the angle of propagation inside the liquid crystal.

We note that Eqs. (70) and (71) implicitly require the phase shift δ between the interference patterns on the top and the bottom surfaces through Eqs. (58) and (59). In the zero-

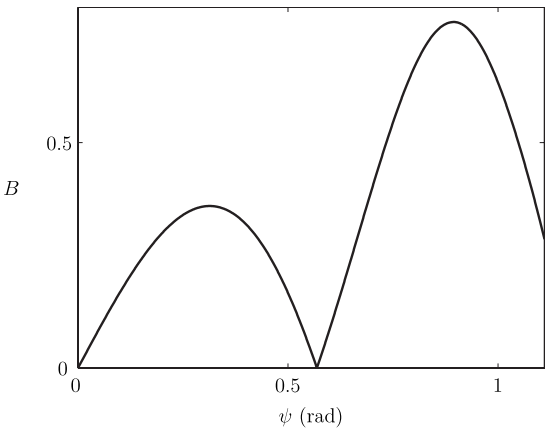

FIG. 6. Functional dependence of the phase modulation parameter B as a function of the internal angle ψ. Fixed parameters: $\mu=6$ and $\Phi_1/\Phi_0=1$.

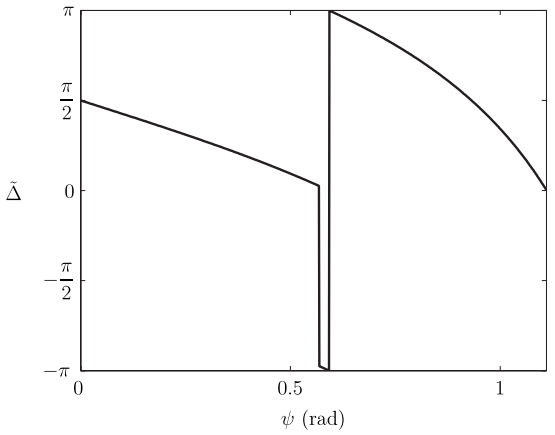

FIG. 7. Functional dependence of the phase modulation parameter $\tilde{\Delta}$ as a function of the internal angle. Other parameters are fixed: $\mu=6$ and $\Phi_1/\Phi_0=1$. Note the discrete jump in $\tilde{\Delta}$ of π, the origin of which is discussed in the text.

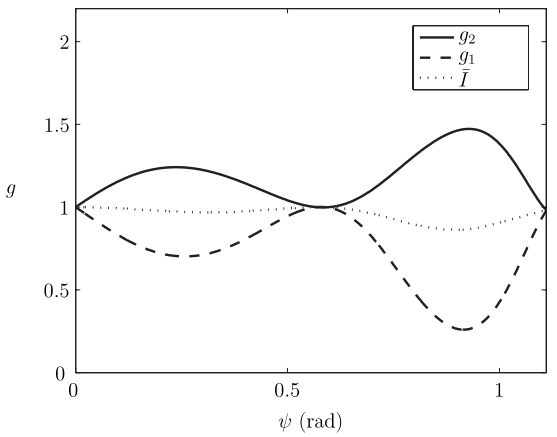

FIG. 8. Energy exchange between beams as a function of the internal angle ψ. Solid line: gain of probe beam. Dashed line: gain of pump beam. Dotted line: $\bar{I}$ [see Eq. (74)] represents the degree of energy conservation in the system. Fixed parameters: $\mu=6$ and $\Phi_1/\Phi_0=1$.

order approximation this quantity can be expressed from Eq. (8) as follows:

$$\delta = -2|k|L \sin\psi \sin\gamma = -\sqrt{\frac{\varepsilon_\parallel}{\varepsilon_\perp}}\mu \tan\psi. \tag{75}$$

The principal result from Fig. 6 is that $B<1$ everywhere, which implies that for all intents and purposes only transmitted and first order diffracted beams occur. In Fig. 7 we plot $\tilde{\Delta}(\psi)$. It can be seen from Eq. (69) that the phase modulation parameter $\tilde{\Delta}$ governs the sign of the energy exchange. For $0<\tilde{\Delta}<\pi \sin\tilde{\Delta}>0$, and the probe beam is amplified by the pump beam. However, for $\pi<\tilde{\Delta}<2\pi \sin\tilde{\Delta}<0$ and the pump beam is amplified. In Fig. 6, $B(\psi)=0$ for $\psi\approx 0.57$. At this point the quantities A [Eq. (58)] and C [Eq. (59)] are both equal to zero and change sign. This implies a sudden phase shift of π in the phase modulation parameter $\tilde{\Delta}$, which indeed occurs at $\psi\approx 0.57$ and at $\psi\approx 0.59$ in Fig. 7.

The behavior of the gain is shown in Fig. 8. Maximal gain is achieved when $\sin\tilde{\Delta}(\psi)=1$, corresponding to $\psi\approx 0.93$ [see Eqs. (69) and (73)]. At $\psi=0$ the gain $g(\psi)=1$. We also note that at this point, from the symmetry of the system there is no energy exchange. The quantity $\bar{I}$ plotted on this graph is almost unity everywhere. This means that there are only small energy losses; the incident energy is mainly distributed between the outgoing probe and pump beams.

In Fig. 9 we plot the pump beam diffraction efficiency. This measures the proportion of energy diffracted from the pump beam in the probe beam direction. The diffraction efficiency η is a function only of B [Eq. (71)]. The maximum possible diffraction efficiency is given by $\eta(B)\approx 0.338$ at $B\approx 1.83$. This maximum value does not depend on the details of our model and remains true for thin gratings [19]. But in Fig. 9, the maximum value of diffraction efficiency $\eta\approx 0.13$ occurs at $\psi\approx 0.89$. The discrepancy between the theoretical maximum and this maximum can be ascribed to the fact that $B(\psi)<1$ everywhere.

We now turn to the study of energy exchange as a function of the angle between interfering beams. Increasing the angle 2γ between beams increases the non-dimensional wave vector $\mu=\tilde{q}L$. Quantitatively, choosing parameters given in Table I, we find that for $\gamma\approx 2.4°$, $\mu\approx 6$. We examine the dependence $g(\mu)$ for $\psi=0.93$, i.e. at the maximum of g appropriate to Fig. 8. The dependence of the gain on μ is shown in Fig. 10. For $\mu<5$, B is larger than unity [see inset (a)] and $\bar{I}<1$ [see Eq. (74)] is less than unity. In this regime there is considerable energy loss due to probe beam diffraction into diffraction orders of order $n>1$. However, for $\mu>5$, $B<1$ and the quantity $\bar{I}$ is close to 1. In this regime energy is conserved. The maximal gain is achieved at $\mu\approx 6$. This maximum is consistent with our results from Figs. 6–9.

In Fig. 11 we plot the diffraction efficiency η. The maxima of 0.338 occur at $\mu\approx 0.5$ and $\mu\approx 1.6$, corresponding to maxima in the Raman-Nath regime [20]. But these maxima occur for $\mu<5$, where as we have seen above, there is considerable diffractive energy loss. The physical relevant

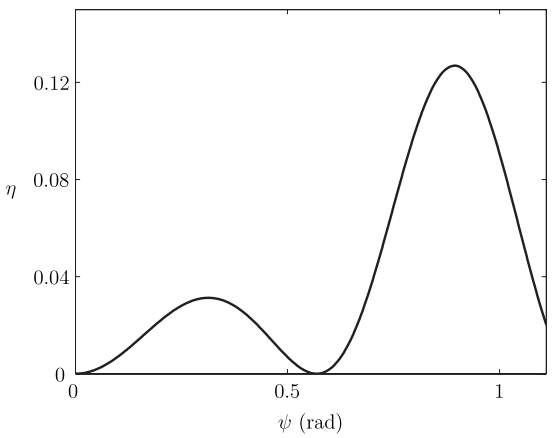

FIG. 9. The dependence of diffraction efficiency η on the internal angle ψ. Fixed parameters: $\mu=6$ and $\Phi_1/\Phi_0=1$.

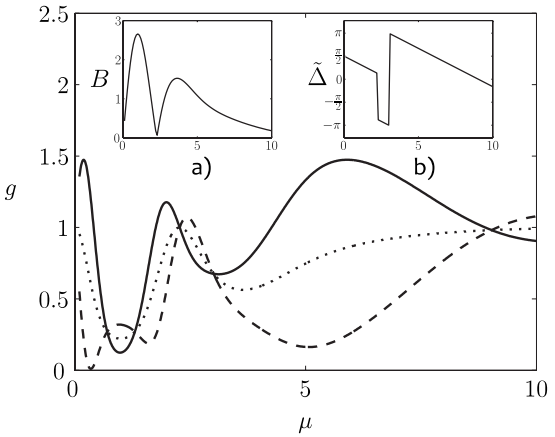

FIG. 10. Energy exchange between beams as a function of μ, the nondimensional grating wave vector. Solid line: gain of probe beam. Dashed line: gain of pump beam. Dotted line: $\bar{I}$ (see Fig. 8). (a) Phase modulation amplitude B as a function of μ; (b) phase modulation parameter $\tilde{\Delta}(\mu)$. Fixed parameters: ψ=0.95 and Φ_1/Φ_0=1.

maximum occurs for $\mu \approx 4$. Here the diffractive energy loss is much reduced, although some energy loss still remains.

The strength of the grating modulation [Eq. (26)] depends on the ratio $\frac{\Phi_1}{\Phi_0}$. In all our previous plots (Figs. 6–11) we have set the ratio $\frac{\Phi_1}{\Phi_0}=1$. This ratio can be modified in two ways. In principle, one can change Φ_1 by changing the surface preparation. Alternatively (and more simply) one can apply an external voltage Φ_0 across the liquid crystal. Here we suppose Φ_1 and Φ_0 to be independent quantities.

We now investigate the effect of external voltage on the energy exchange for $g(\psi=0.93, \mu=6)$. This corresponds to the point (see Fig. 8), where g is maximal with respect to varying ψ with other parameters as taken in Table I. The optical modulation is a strong function of the director modulation. It is thus useful to analyze the director modulation as a function of external applied field.

We first make a quantitative analysis of the behavior of the director modulation as a function of voltage. The liquid

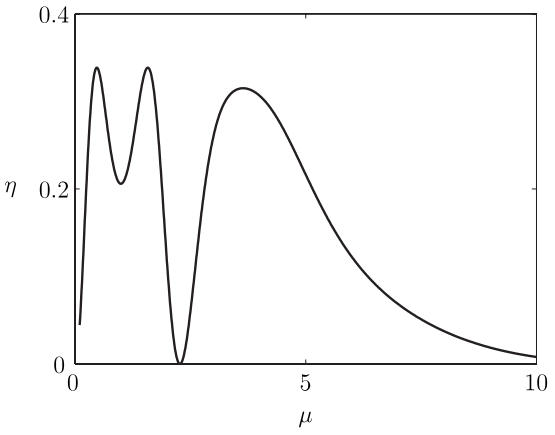

FIG. 11. The dependence of diffraction efficiency η on the nondimensional wave vector μ. Fixed parameters: ψ=0.93 and Φ_1/Φ_0=1.

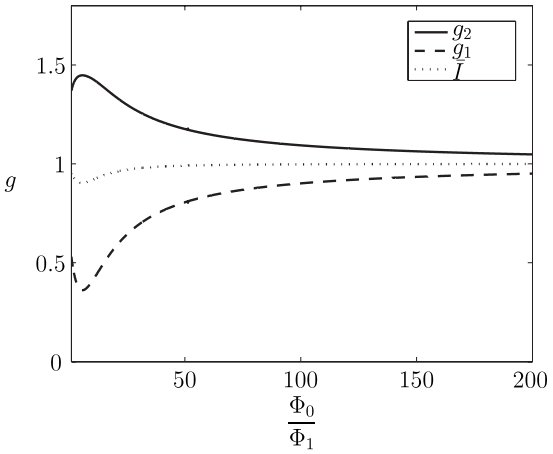

FIG. 12. Dependence of gain of probe beam as a function of $\frac{\Phi_0}{\Phi_1}$. This is equivalent to increasing the external field. Note that the abscissa starts at 1, the lowest value for which our treatment is valid, although the difference between 1 and 0 is not visible on this scale. Further structure may occur in the region $\frac{\Phi_0}{\Phi_1} \leqslant 1$.

crystal director distribution is given by Eq. (26).

$$\theta(x,z) = -qL\frac{\Phi_1}{\Phi_0}\left[\cos\frac{\delta}{2}\sin\left(qx+\frac{\delta}{2}\right)\left\{\frac{\cosh\mu\sigma}{\cosh\mu/2}-\frac{\cosh\kappa\sigma}{\cosh\kappa/2}\right\}\right.$$
$$\left.+\sin\frac{\delta}{2}\cos\left(qx+\frac{\delta}{2}\right)\left\{\frac{\sinh\mu\sigma}{\sinh\mu/2}-\frac{\sinh\kappa\sigma}{\sinh\kappa/2}\right\}\right], \quad (27')$$

The voltage enters this expression explicitly through the multiplier $\frac{\Phi_1}{\Phi_0}$, and implicitly through the quantity κ, where $\kappa^2=\mu^2+\nu^2$, $\nu=\frac{L}{\xi}=\Phi_0(\frac{\varepsilon_a}{K})^{1/2}$ is a rescaled voltage.

In the limit of high voltages, the κ term in Eq. (26) can be neglected, and hence the reorientation $\theta(x,z) \propto \Phi_0^{-1}$. Hence at high voltages the director approaches a uniform distribution, in which case the beam coupling disappears and $g=1$. In our approximation, the low voltage limit $\Phi \to 0$ is inaccessible; the minimum voltage for which our approximations are valid is $\Phi_0 \approx 1$. This follows because we have assumed that the modulated component of the electric field is small by comparison with the external field in the derivation of the liquid crystal director distribution (23). The dependence of gain on the external potential is shown in Fig. 12. For $\Phi_0=1$ $g \approx 1.3$. The gain reaches a maximum $g \approx 1.44$ at $\Phi_0 \approx 7$. For $\Phi_0 > 7$ the energy exchange parameter g decreases monotonically toward a value of unity (i.e., no energy exchange) in the high potential limit.

VI. DISCUSSION AND CONCLUSIONS

In this paper we have carried out a model phenomenological calculation of energy exchange between beams incident on a thin liquid crystal grating sandwiched between two photoconducting layers. In this model calculation, the liquid crystal is subject to homeotropic boundary conditions, but this is not an essential feature of the model. The energy exchange involves diffraction by an induced grating, with the exchange occurring when each incident wave is diffracted

into the outgoing path of the other. We find that there is a regime in which significant energy exchange can occur, without leakage into other higher order diffracted waves. There is also another regime in which such leakage does occur.

We find a maximal gain of $g=1.45$, which occurs for a grating wavelength of the order of the thickness of the sample. This appears to be a robust result, and qualitatively consistent with experiment [31]. The robustness of this result is consistent with calculations by Sarkissian *et al.* [32]. These authors obtain a similar theoretical result for a system in which there is a modulation of the surface anchoring potential, rather than of the surface electric potential. There is also significant dependence on the bulk voltage. In the limit of high voltage there is no effect (because there is no director modulation and hence no grating). As the voltage is reduced the effect increases. Our calculation does not permit the evaluation of the low-voltage limit, but we do find a maximum when the ratio of the external voltage to the surface modulation is about 10. Unfortunately the phenomenological nature of our calculation does not permit us to make any quantitative predictions with respect to actual voltage or beam intensities required to achieve this. However, the gain maximum as a function of voltage is also manifested as a maximum with respect to varying beam intensity. Although this calculation is vague with respect to quantitative prediction, we believe that the existence of a maximum as a function of voltage is a qualitatively robust result.

The calculation is broken down into a number of parts. First we have supposed that interference between the incident beams affects the photoconducting layers by only changing the electric potential at the boundaries of the sample, and does so in proportion to some power of the beam intensities. Secondly we have calculated the modification of the electric field inside the liquid crystal sample, supposing that there is a zeroth order field due to some imposed bulk potential. Thirdly, we have used the electric field to calculate the modulated director distribution, which necessarily then acts as an optical grating. Fourthly, we have investigated the transmission of each beam through the modulated liquid crystal layer using a WKB-like approximation in the spirit of geometrical optics. The result of this calculation is a phase and amplitude optical profile for the extraordinary wave along the outgoing surface. Finally, using this surface optical profile we have used the Kirchoff method to evaluate the far field, and hence diffraction and interbeam energy exchange.

The strategy is in the spirit of the standard Raman-Nath calculation. However, the standard calculation cannot be used here, because the existence of inhomogeneities in the dielectric function perpendicular to the grating direction complicates the calculation. But nevertheless the resulting expression for the intensity of the diffracted beams of different orders retains features of the analogous Raman-Nath regime calculation for thin grating diffraction [20].

Some features of our calculation are simplified in order to make the problem tractable. We have measured the potential induced at the surface with respect to the bulk voltage across the cell. An alternative low external voltage expansion would also, in principle, be possible, but we have not pursued this approach here. In addition, we have solved the liquid crystal director in a one-elastic-constant approximation, and also linearized the Euler-Lagrange equations coupling the director and the electric potential. Neither of these approximations is essential, but there are significant potential advantages in obtaining analytic formulas in what could otherwise be a computational minefield. The optical scattering in the system itself implies that the picture in which the incident beams penetrate the liquid crystal layer unimpeded to provide potential modulations at the outgoing surface is only the first step in an iterative procedure. While it is possible to carry out this iteration in our model, we have chosen not to do so. This is partly because we would lose what analytic simplification we have achieved. Also, however, given that we only have a phenomenological model, we would in any case be no closer at this stage to a quantitative comparison with experiment.

One particularly interesting feature of our calculations is that we are able to identify separately components of the refractive index modulation which are respectively in-phase and out-of phase with the mean optical field intensity. It is often stated that if the refractive index and optical field modulations are in-phase with respect to each other, then no two-beam coupling would be expected. Within the usual theory of photorefraction, this result is robust. Normally the energy transfer term in the coupled wave equations disappears in the in-phase case.

However, notwithstanding the inaccuracies and approximations involved in our calculations, we find that in our case this statement is unambiguously false. The in-phase beam coupling is indeed lower, but no by means identically zero. This is surprising, given the comment above about the robustness of the result. We have not yet been able to carry out a detailed analytic comparison between our case and the standard Raman-Nath and Bragg regimes. However, it is not obvious that the analogy between the standard cases and the case considered in this paper is as close as one might think. In the standard case, which applies everywhere in the literature, the nonlinearity is internal to the system. By contrast, surface-mediated photorefraction is precisely that. There is an extra feature in the system not found elsewhere. This involves effectively a long-range interaction, and the structure of the analysis in the Bragg regime is consequently changed in an essential way. From this point of view, the breakdown of the (in-phase intensity and refractive index modulations=no coupling) result is less surprising.

Nevertheless, a puzzle remains, to which we hope to return in future work. One further remark may be relevant. The apparent difference between our results and the widely held view seems to depend on the precise definition of what is meant by "gain." In this paper, gain is defined as the degree of amplification. In the model we present, the amplification of the probe beam is due to the diffraction at the thin grating, with a maximum value $\sim 34\%$.

The underlying cause of all amplification in this model is the constructive interference between the diffracted component of the pump beam, and the probe beam. As a result, it is, of course, not possible to transfer all energy from the pump to the probe beam. But the process we describe differs essentially from energy exchange in thick gratings. Thick-grating energy exchange is a bulk, rather than a surface phe-

nomenon. Now the gain exponentially increases with the thickness of the grating. As a consequence, it is in this case possible to transfer all energy from the pump to the probe beam.

Although we have been able to obtain a semianalytic form for the beam coupling, the calculation is complicated. It involves electric fields, director distributions and light transmission through an inhomogeneous medium. The result is that the final magnitude of the effect under consideration seems to bear no simple relation to the rather large number of parameters which enter the problem. We can say definitively that the external voltage, the angle of incidence, the angle between the two beams, not to mention the thickness of the cell and the liquid crystal elastic constants, all play an important role, and furthermore the response is not monotonic. From an engineering point of view, there are clearly several possible ways to control the energy exchange process.

But apart from the pronounced maximum in beam coupling when the grating width is of the order of the thickness of the sample, we are unable at this stage to make further robust comments concerning the functional relationships without resorting to specific calculations. We cannot say whether further studies, and in particular a reliable microscopic theory, will clarify the situation.

The theory presented in this paper can be developed in a number of ways. It can be trivially extended to liquid crystal cells in which only a single photoconductive layer attached. Alternatively, we might extend the present work, involving homeotropic surfaces, to low voltages, or to liquid crystal cells with homogeneous boundary conditions. Such a theory would be applicable, for example, to the experiments of Pagliusi and Ciparrone [33]. We also note that in this paper, the director distribution throughout the sample is clustered around the homeotropic direction. However, one might expect intuitively that the most dramatic effects would occur when the voltage modulation and the external field conspire to produce large director shifts between one part of the sample and another. Our framework may permit such a calculation.

The main weakness of the theory concerns the nature of the relationship between the potential modulations Φ_1 and the beam intensities. The lack of relevant experimental data is partly because, as far as we are aware, the present paper is the first suggestion that the main mechanism for photorefractive beam coupling involves this quantity. We are hopeful that future work will therefore remedy this deficiency. An experiment which measures this quantity might involve Frederiks transition measurements in the presence of an externally applied optical beam.

At a later stage, we would also hope to make contact between this theory and a more microscopic theory which elucidate processes in the photoconductive media, and at the photoconductive layer-liquid crystal interface. A second weakness involves the geometric optics approximation, and this restricts our calculations to the short wavelength limit. In most liquid crystal cells, this will be sufficient, but in principle longer-wavelength corrections are interesting. Indeed, we are currently carrying out optical calculations in which the optics is treated by solving the Maxwell equations exactly. Such a scheme will automatically permit a self-consistent solution of the optics-potential-elastic problem.

ACKNOWLEDGMENTS

This work has been partially supported by a Royal Society Joint Project Grant "Modelling the electro-optical properties of ferroelectric nematic liquid crystal suspensions" (T.J.S. and V.Y.R.), a NATO Grant No. CBP-.NUKR.CLG.981968 "Electro-optics of heterogeneous liquid crystal systems," and an INTAS award No. 1000019-6375 (V.O.K.). We also gratefully acknowledge discussions with Dr. Malgosia Kaczmarek and Dr. Giampaolo D'Alessandro (Southampton), Professor Anatoli Khizhnyak (Metrolasers, California), and Professor Ken Singer (Cleveland, USA).

APPENDIX: LIGHT-INTENSITY-INDUCED MODULATION OF SURFACE POTENTIALS

In Sec. II, we have discussed the response of the surface potential to the incident beam interference pattern. Specfically, we propose in Eq. (9):

$$\varphi(z=0,x) = -\Phi_0/2 + \Phi_1 \cos qx,$$

$$\varphi(z=L,x) = \Phi_0/2 + S\Phi_1 \cos(qx+\delta), \tag{A1}$$

with $S=\pm 1$, and where the sign of S depends on the detailed physical picture adopted to model the relevant surface physics.

A number of mechanisms have been discussed in the literature which link a surface potential response to a beam intensity pattern in the surface region. In this appendix we examine two physical scenarios which may illuminate the microscopic surface physics. Specifically, we will thus be able to gain insight into the correct determination of the parameter S. We first examine a mechanism for grating formation which follows closely, though not exactly, a model introduced by Ono [9]. The key features of this model are as follows.

The photoconductive polymer layer is a semiconductor with a band gap. This layer is illuminated by the optical interference pattern. The optical beam excites mobile holes and electrons close to the band edges. These are known as photocarriers or photocharges. The optical interference pattern thus involves a spatial modulation of these photocarriers. The photocharges leak into the liquid crystal, where the equilibrium density remains periodically modulated. The result is a modulated space-charge field, which reorients the liquid crystal director field. For this mechanism, the charge modulation on the bottom and top surfaces possess the same sign, and in this case $S=+1$. We adopt this convention in Eq. (9).

However, Pagliusi and Chipparone [12] discuss an alternative mechanism. In this picture, the principal role is played by ions present in liquid crystal. When an external electric field is applied, the ions move toward the electrodes of opposite polarity. This causes thin charged layers to form near

the electrodes. As before the modulated incident optical intensity induces a modulated photocarrier distribution inside the photoconductive layer. Now, however, these charges recombine with the charges in the charged layers, but the pattern of recombination is periodically modulated. The rsult is a net charge modulation, which leads to a space-charge field. Now the charge modulation on the top and bottom boundaries possess opposite signs, and hence in this case $S=-1$ in Eq. (9).

Thus, in the absence of a detailed physical picture of the mechanism of the potential modulation, no definitive statement can be made concerning the sign of S. It seems likely, however, that an experimental determination might be possible.

[1] I. Khoo and S. Wu, *Optics and Nonlinear Optics of Liquid Crystals* (World Scientific, Singapore, 1993).
[2] G. P. Wiederrecht, Annu. Rev. Mater. Res. **31**, 139 (2001).
[3] I. Janossy, J. Nonlinear Opt. Phys. Mater. **8**, 361 (1999).
[4] L. Lucchetti, M. Gentili, and F. Simoni, Opt. Express **14**, 2236 (2006).
[5] A. Miniewicz, S. Bartkiewicz, and J. Parka, J. Opt. Commun. **149**, 89 (1998).
[6] A. Miniewicz, K. Komorowska, J. Vanhanen, and J. Parka, Org. Electron. **2**, 155 (2001).
[7] S. Bartkiewicz, A. Miniewicz, F. Kajzar, and M. Zagorska, Mol. Cryst. Liq. Cryst. Sci. Technol., Sect. B: Nonlinear Opt. **21**, 99 (1999).
[8] M. Kaczmarek, J. Appl. Phys. **96**, 2616 (2004).
[9] H. Ono and N. Kawatsuki, Opt. Commun. **147**, 237 (1998).
[10] J. Zhang, V. Ostroverkhov, K. Singer, V. Reshetnyak, and Y. Reznikov, Opt. Lett. **25**, 414 (2000).
[11] P. Pagliusi and G. Cipparrone, Appl. Phys. Lett. **80**, 168 (2002).
[12] P. Pagliusi and G. Cipparrone, Phys. Rev. E **69**, 061708 (2004).
[13] H. Kogelnik, Bell Syst. Tech. J. **48**, 2909 (1969).
[14] P. Yeh, *Introduction to Photorefractive Non-linear Optics* (Wiley, New York, 1993).
[15] R. Collier, C. Burckhardt, and L. Lin, *Optical Holography* (Academic Press, New York, 1971).
[16] G. Montemezzani and M. Zgonik, Phys. Rev. E **55**, 1035 (1997).
[17] G. Montemezzani and M. Zgonik, in *Photorefractive Materials and their Applications 1*, edited by P. Günter and J.-P. Huignard (Springer, Berlin, 2006), Chap. 4, pp. 83–116.
[18] A. V. Galstyan, G. G. Zakharyan, and R. S. Hakobyan, Mol. Cryst. Liq. Cryst. **453**, 203 (2006).
[19] J. Goodman, *Introduction to Fourier Optics* (Mc Graw Hill, New York, 1996), Chap. 7.
[20] C. V. Raman and N. S. N. Nath, Proc. Indian Acad. Sci., Sect. A **2**, 406 (1935).
[21] K. Kojima, Jpn. J. Appl. Phys., Part 1 **21**, 1303 (1982).
[22] N. V. Tabiryan and C. Umeton, J. Opt. Soc. Am. B **15**, 1912 (1998).
[23] P. Korneichuk, Y. Reznikov, O. Tereshchenko, and V. Reshetnyak, Mol. Cryst. Liq. Cryst. **422**, 27 (2004).
[24] S. Bartkiewicz, A. Miniewicz, F. Kajzar, and M. Zagorska, Appl. Opt. **37**, 6871 (1998).
[25] G. Panasyuk, J. Kelly, E. C. Gartland, and D. W. Allender, Phys. Rev. E **67**, 041702 (2003).
[26] T. C. Kraan, T. van Bommel, and R. A. M. Hikmet, J. Opt. Soc. Am. A **24**, 3467 (2007).
[27] Yu. A. Kravtsov and Y. I. Orlov, *Geometrical Optics of Inhomogeneous Media* (Springer Verlag, Berlin, 1990).
[28] M. Abramowitz and I. A. Stegun, *Handbook of Mathematical Functions, with Formulas, Graphs, and Mathematical Tables*, 9th ed. (New York, Dover, 1972), Chap. 9.1.
[29] M. Born and E. Wolf, *Principles of Optics*, 6th ed. (Pergamon Press, New York, 1980), Chap. 8.
[30] A. Yariv and P. Yeh, *Optical Waves in Crystals: Propagation and Control of Laser Radiation* (Wiley, New York, 1984).
[31] I. C. Khoo, IEEE J. Quantum Electron. **32**, 525 (1996).
[32] H. Sarkissian, N. Tabirian, B. Park, and B. Zeldovich, Mol. Cryst. Liq. Cryst. **451**, 1 (2006).
[33] P. Pagliusi and G. Cipparrone, J. Opt. Soc. Am. B **21**, 996 (2004).
[34] We might imagine a system in which the boundary conditions were homogeneous, for example, and only one surface was attached to a photosensitive layer. Only one of the surfaces would then be affected by an incident light beam. A single light beam would then affect the effective voltage across the cell. The effect would be proportional to the light intensity, and the constant of proportionality would be the parameter σ. The magnitude of the effect could be measured by monitoring the critical Frederiks field.
[35] This equation is a derivative of what in the literature is usually known as the eikonal equation.